ARTICLE

Electron Transfer Theory Revisit: Motional Narrowing Induced Non-Markovian Rate Processes[†]

Ying Chen[a], Rui-xue Xu[a], Hong-wei Ke[b], Yi-jing Yan[a,b*]

a. Hefei National Laboratory for Physical Sciences at Microscale, University of Science and Technology of China, Hefei 230026, China;
b. Department of Chemistry, Hong Kong University of Science and Technology, Hong Kong

While the exact theory of chemical reaction rate processes is always non-Markovian, experimental rates do often show practically Markovian that supports kinetics rate constant description. In this work, we propose to use the Kubo's motional narrowing line shape function to characterize the Markovian character of the simplest two-state electron transfer reaction system. On the basis of analytical results, we demonstrate the related Markovianicity parameter as an interplay between the fluctuating solvent environment and the coherent transfer coupling. It is found that a non-Markovian rate process is most likely to occur in a symmetric system in the fast solvent modulation regime, where the resonant tunneling enhancement plays the important role. The effect of quantum solvation on electron transfer, which is dominant in the fast modulation regime, will also be highlighted.

Key words: Non-markovian rate, Quantum solvation, Electron transfer

I. INTRODUCTION

The fluctuation and interaction of solvent environment plays a pivotal role in chemical reactions. Consider a simple two-state $a \rightarrow b$ reaction. From the theoretical point of view, an exact construction of the rate equation, via either the projection operator approach [1-3] or the reduced density matrix formalism [4-6], leads always to a generalized rate equation,

$$\dot{P}_a(t) = -\int_0^t d\tau \hat{k}(t-\tau)P_a(\tau) + \int_0^t d\tau \hat{k}'(t-\tau)P_b(\tau) \quad (1)$$

Here, $\hat{k}(t)$ and $\hat{k}'(t)$ denote the forward and backward rate memory kernels. On the other hand, one often finds in practice that the simple kinetic equation, within the Markovian rate constant description (cf. Eq.(11) and Eq.(12)),

$$\dot{P}_a(t) = -k_0 P_a(t) + k_0' P_b(t) \quad (2)$$

can well describe the observed rate process. The resulting reactant population $P_a(t)$ decays exponentially toward its equilibrium value at a given temperature. Is there any quantitative justification for the Markovian rate processes being often observed experimentally? Also, if the solvent motion gets faster, whether the rate process appears more Markovian or less?

In this work, we try to address the issues on the Markovian character of elementary rate process. The

theoretical analysis will be made in connection to the electron transfer (ET) rate theory. In due course we will also discuss about the effects of quantum solvation and motional narrowing on ET rate processes.

II. ELECTRON TRANSFER RATE THEORY: EFFECT OF MOTIONAL NARROWING

The research in the field of ET rate theory has grown enormously since 1950s [1-21]. The standard ET system–bath model Hamiltonian reads

$$H_{\mathrm{T}} = h_a|a\rangle\langle a| + (h_b + E^\circ)|b\rangle\langle b| + V(|a\rangle\langle b| + |b\rangle\langle a|) \quad (3)$$

here, E° denotes the reaction endothermicity, V the transfer coupling matrix element, and h_a (h_b) the solvent Hamiltonian for the ET system in the donor (acceptor) state. The system is initially in the donor $|a\rangle$ site, with the solvent (bath) equilibrium density matrix $\rho_a^{\mathrm{eq}} \propto e^{-h_a/(k_B T)}$ at the specified temperature T.

A nonperturbative rate theory can be generally constructed via the reduced density matrix dynamics [4-6]. The involving dissipative memory kernels can be expressed in terms of the continued fraction formalism [22,23]. This formalism can further be evaluated analytically for ET in Debye solvents; see the Eq.(36) with Eqs.(24)-(29) of Ref.[4]. Those analytical results will be used in the later numerical demonstrations on the ET rates in both adiabatic and nonadiabatic regimes.

To illustrate some basic features, let us start with the nonadiabatic rate process, in which the rates are proportional to V^2. The standard perturbation theory

leads to (setting $\hbar \equiv 1$)

$$\hat{k}_{\text{NA}}(t) = 2V^2 \text{Re} \left\{ \exp[-g(t)] \right\} \quad (4)$$

$$\exp[-g(t)] = \left\langle \exp_+ \left\{ -i \int_0^t d\tau \, [E^\circ + U(\tau)] \right\} \right\rangle \quad (5)$$

Here, $U(\tau) \equiv e^{ih_a\tau} U e^{-ih_a\tau}$ is the solvation coordinate, $U \equiv h_b - h_a$, in the solvent h_a-interaction picture. It is a stochastic bath operator, involving in Eq.(5) with the solvent ensemble average, $\langle \cdot \rangle \equiv \text{tr}_B(\cdot \rho_a^{\text{eq}})$. Apparently, the solvation coordinate describes the energetic fluctuation following the ET from the donor $|a\rangle$ to the acceptor $|b\rangle$ site. Assume the fluctuation follows a Gaussian statistics. The solvation effect on the ET can be completely characterized by the solvation energy,

$$\lambda \equiv \langle h_b - h_a \rangle = \langle U \rangle \quad (6)$$

and the solvation correlation function,

$$C(t) = \langle [U(t) - \lambda][U(0) - \lambda] \rangle \quad (7)$$

The nonadiabatic rate kernel expression, Eqs.(4) and (5), can now be completed by using the second-order cumulant expansion that is exact for the Gaussian solvation process [1-3,12-20].

$$g(t) = i(E^\circ + \lambda)t + \int_0^t d\tau \int_0^\tau d\tau' C(\tau') \quad (8)$$

Note that $U(t)$ is an operator in the stochastic bath space, it in general does not commute with $U(t=0)$. Thus, the quantum solvation correlation is a complex function. Its real and imaginary parts are related by the fluctuation-dissipation theorem. For example, the correlation function for a Debye solvent in finite temperature reads

$$C(t > 0) = \lambda(2k_{\text{B}}T - i\tau_{\text{L}}^{-1})e^{-t/\tau_{\text{L}}} \quad (9)$$

The longitudinal relaxation time τ_{L} relates to the Debye time [1-3] as $\tau_{\text{L}} = (\varepsilon_\infty/\varepsilon_0)\tau_{\text{D}}$, by which the Debye dielectric function reads $\varepsilon(\omega) = \varepsilon_\infty + (\varepsilon_0 - \varepsilon_\infty)/(1 + i\omega\tau_{\text{D}})$.

In comparison, the classical treatment of solvation assumes $U(t)$ as a classical stochastic variable, and thus $C_{\text{cl}}(t)$ is real. For the Debye model (Eq.(9)), the classical solvation limit is reached when $\tau_{\text{L}} \gg \tau_{\text{ther}} \equiv (k_{\text{B}}T)^{-1}$. Note that τ_{L} is approximately proportional to the solvent viscosity [1-3]. Thus $\tau_{\text{L}} \gg \tau_{\text{ther}}$ and $\tau_{\text{L}} \ll \tau_{\text{ther}}$ will be termed later also as the high- and low- viscosity regimes, respectively. The classical treatment of solvation is valid in the high-viscosity regime.

To proceed, let us recast Eq.(1) in the Laplace domain.

$$s\widetilde{P}_a(s) - P_a(0) = -k(s)\widetilde{P}_a(s) + k'(s)\widetilde{P}_b(s) \quad (10)$$

with $\widetilde{P}_j(s) \equiv L\{P_j(t)\}$ and

$$k(s) \equiv L\{\hat{k}(t)\} \equiv \int_0^\infty dt \, e^{-st}\hat{k}(t) \quad (11)$$

The rate constant that describes the decay at the long-time region is given by

$$k_0 \equiv k(s=0) = \int_0^\infty dt \, \hat{k}(t) \quad (12)$$

In particular, the nonadiabatic rate constant can be evaluated as [19,20]

$$k_0^{\text{NA}} = 2V^2 \text{Re} \int_0^\infty dt \, \exp[-g(t)] \quad (13)$$

with $g(t)$ being given in Eq.(8).

In the high-viscosity ($\tau_{\text{L}} \gg \tau_{\text{ther}}$) regime, the solvation correlation $C(\tau')$ in Eq.(8) can be taken as its static limit of $C(\tau') \approx C(0) = 2\lambda k_{\text{B}}T$. The resulting nonadiabatic rate constant reads [7-9]

$$k_0^{\text{NA}} = \frac{V^2}{\sqrt{\lambda k_{\text{B}}T/\pi}} \exp\left[-\frac{(E^\circ + \lambda)^2}{4\lambda k_{\text{B}}T}\right] \quad (14)$$

This is the celebrated Marcus' rate expression. The classical solvation barrier is of $\Delta G_{ba}^* = (E^\circ + \lambda)^2/(4\lambda)$ for the ET reaction, and the inversion occurs at $E^\circ = -\lambda$.

In the low-viscosity regime, more precisely when $\sqrt{2\lambda k_{\text{B}}T}\tau_{\text{L}} \ll 1$ but $\Gamma \equiv 2\lambda k_{\text{B}}T\tau_{\text{L}}$ remains finite, Eq.(8) with Eq.(9) reduces to $g(t) \approx \Gamma t + iE^\circ t$, leading Eq.(13) to

$$k_0^{\text{NA}} = \frac{2V^2\Gamma}{(E^\circ)^2 + \Gamma^2} \quad (15)$$

Apparently, this is the quantum solvation regime [5], where the ET proceeds as a tunneling, with the maximum rate occurring at the Fermi resonance ($E^\circ = 0$). The maximum rate here is much larger than that in the high-viscosity regime. This is closely related to the well-established motional narrowing phenomenon, addressed originally by Kubo in the context of spectroscopy [24,25]. The (Lorentzian) width Γ in the low-viscosity (or fast-modulation) regime is much smaller than the (Gaussian) width $\sqrt{2\lambda k_{\text{B}}T}$ in the high-viscosity (or static) regime. Here, the rate constant is treated as a function of E°, and the total integrated area remains constant.

We will show soon that, as the population dynamics is concerned, the motional narrowing enhanced rate at $E^\circ = 0$ is in favor of a non-Markovian rate process. This seems somewhat counter-intuitive, as the motional narrowing results from a Markovian spectroscopic process [24,25]. For the asymmetric ET system ($E^\circ \neq 0$), the motional narrowing may, however, have the opposite effect. The detailed analysis is as follows.

III. NATURE OF ELECTRON TRANSFER: MARKOVIAN VERSUS NON-MARKOVIAN

From Eq.(1) and the initial condition $P_a(0) = 1$, we have $\dot{P}_a(0) = 0$, and $\ddot{P}_a(0) = -\hat{k}(0) = -2V^2$. The last iden-

tity is inferred from the fact that $\hat{k}(0)$ is in general identical to $\hat{k}_{NA}(0)$, even when the reaction is adiabatic. The scaled population,

$$\Delta(t) \equiv \frac{P_a(t) - P_a(\infty)}{P_a(0) - P_a(\infty)} \qquad (16)$$

should have the short- and long-time asymptotic behaviors as follows.

$$\Delta(t \to 0) \approx e^{-\hat{w}_0 t^2/2}, \quad \Delta(t \to \infty) \approx e^{-w_0 t} \qquad (17)$$

with (noting that $P_a(0)=1$)

$$\hat{w}_0 = \frac{\hat{k}(0)}{P_a(0) - P_a(\infty)} = \frac{2V^2(1 + K_{eq})}{K_{eq}} \qquad (18)$$

$$w_0 = k_0 + k_0' = \frac{k_0(1 + K_{eq})}{K_{eq}} \qquad (19)$$

$K_{eq} \equiv P_b(\infty)/P_a(\infty) = k_0/k_0'$ denotes the reaction equilibrium constant. Note that the rate constant k_0 (or k_0') here is general, not just limited for the nonadiabatic or weak transfer coupling case. However, in the strong transfer coupling regime, $\Delta(t)$ may also be significantly influenced by the coherent motion and exhibit quantum beats. The resulting rate process, strictly speaking, is non-Markovian.

This paper focuses on the Markovian character of the population evolution envelop. The population evolution itself can in general have quantum beats. As the asymptotic behaviors of Eq.(17) are concerned, it may suggest to use again the Kubo's line shape function [24,25],

$$\Delta_K(t) = \exp\left[-\kappa^{-2}\left(e^{-\hat{w}_0 t/w_0} - 1 + \frac{\hat{w}_0 t}{w_0}\right)\right] \qquad (20)$$

to analyze the nature of population transfer dynamics. The involving Kubo's Markovianicity parameter is (cf. Eqs.(17)-(19))

$$\kappa \equiv \frac{\hat{w}_0^{1/2}}{w_0} = \left(\frac{2K_{eq}}{1 + K_{eq}}\right)^{1/2} \frac{V}{k_0} \qquad (21)$$

The rate process assumes Markovian or non-Markovian, when $\kappa > 1$ or $\kappa < 1$, respectively.

In the next section, we will show that the Markovian condition holds in the most region of the parameter space. This accounts for why most experiments do exhibit Markovian kinetics rate processes of $\Delta_{Mar}(t) = e^{-w_0 t}$. However, non-Markovian processes can occur in the case of small τ_L and $E^\circ = 0$, where the aforementioned motional narrowing enhanced reaction rate plays the role.

IV. NUMERICAL DEMONSTRATIONS AND DISCUSSION

A. Effect of solvent viscosity

The following numerical demonstrations are made on the basis of the Debye solvent model (Eq.(9)), using the continued fraction formalism of quantum dissipation theory in Ref.[4]. The analytical expressions presented there for the resolutions of both the rate kernels and the reduced dynamics are exact for the Debye solvation model, valid for arbitrary strength of transfer V-coupling. We set $T=298$ K, which amounts to $\tau_{ther}=1/(k_B T) \approx 26$ fs.

It had been demonstrated in Ref.[5] that the solvent viscosity is closely related to the quantum solvation nature. The smaller the viscosity (i.e. the faster the solvent modulation) is, the more important the quantum nature will be. The profound quantum solvation effect has been highlighted for the symmetric ($E^\circ=0$) and classical-barrierless ($E^\circ=-\lambda$) ET systems [5]. In this subsection, we shall first review this issue, and then elaborate its implication to the Markovian character in the aforementioned two representing ET systems. The solvent reorganization energy chosen in this subsection is $\lambda=3$ kJ/mol.

Figure 1 depicts the rate constant $k_0 = k(s)|_{s=0}$ as function of τ_L, evaluated at the specified values of V and E°. This figure is the Kramers' plot. In his seminal study of the dependence of the isomerization reaction rate on the solvent viscosity [26], Kramers treated the reaction as a classical particle crossing a potential barrier, on the basis of classical Brownian motions. In relation to the present work, the celebrated Kramers'
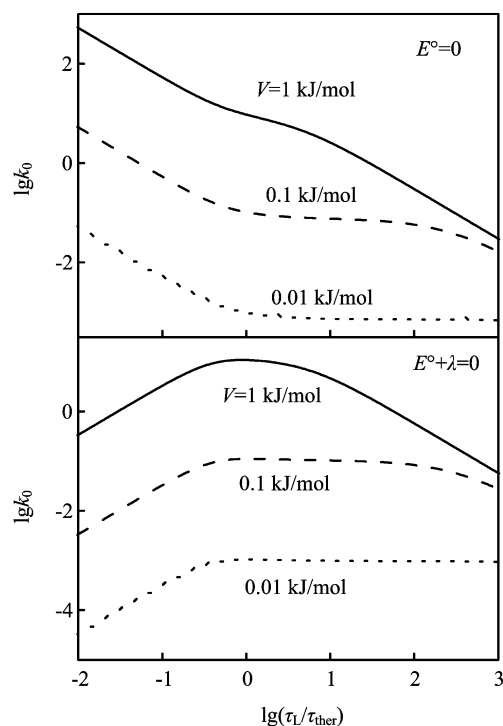

FIG. 1 Electron transfer rate constant k_0 as function of the scaled solvent longitudinal relaxation time τ_L/τ_{ther}, evaluated for $E^\circ=0$ (upper-panel) and $E^\circ+\lambda=0$ (lower-panel), together with the specified transfer coupling strength V along each curve, $\lambda=3$ kJ/mol and $T=298$ K.

fall-off behavior [26,27] can be obviously observed in the strong transfer coupling (V=1 kJ/mol) case; see the solid curves in both of the E°-panels of Fig.1 in the high viscosity ($\tau_L > \tau_{ther}$) regime. This is the well-established diffusion limit of classical reaction rate: the higher the solvent viscosity is, the more the backscattering (or barrier-recrossing) events will be. As V gets smaller, the backscattering is suppressed gradually, leading to the plateau in the dot-curve in each of the E°-panels in Fig.1. This plateau feature can also be inferred from the Marcus' nonadiabatic rate expression, Eq.(14).

In the low-viscosity ($\tau_L < \tau_{ther}$) regime, the quantum solvation shows a distinct ET mechanism from the classical solvation, in either the E°=0 or $E^\circ + \lambda$=0 case of study [5]. The ET is dominant by the Fermi-resonant tunneling in the case of E°=0, while it is barrier-crossing event when $E^\circ + \lambda$=0. In the latter case, the classical ET rate theory such as Eq.(14) is associated with a barrierless reaction [5].

We are now in the position to examine the Markovian character of the ET process. The key quantity here is the Markovianicity parameter κ (Eq.(21)). It involves both the reaction equilibrium constant K_{eq} and the forward reaction rate constant k_0. The detailed knowledge on how K_{eq} depends on the Debye solvent parameters can be found in Ref.[4]. For the rate constant, it is interesting to notice the fact that $k_0 \propto V^2$ in the low-viscosity regime, for the range of transfer coupling strength considered in Fig.1. It implies that the rate constant there can be well approximated by its nonadiabatic counterpart, i.e., Eq.(15) with $\Gamma = 2\lambda k_B T \tau_L$. Thus, when E°=0 and $\tau_L \ll \tau_{ther}$

$$\kappa = \lambda k_B T \tau_L / V \qquad (22)$$

this can be used to estimate the Markovianicity parameter for a symmetric ET system (E°=0, implying also K_{eq}=1) in the low-viscosity regime.

Figure 2 shows the evaluated values of Markovianicity κ (Eq.(21)) associated with the ET systems of Fig.1. For $E^\circ = -\lambda$ (lower-panel), the ET rate process behaves Markovian ($\kappa > 1$), even for the strong transfer coupling (V=1 kJ/mol) case considered here. Apparently, the non-Markovian ($\kappa < 1$) rate process is most likely to occur in the Fermi-resonance tunneling regime, where E°=0 and $\tau_L \ll \tau_{ther}$, with the approximated expression of κ given as Eq.(22).

Figure 3 depicts the scaled population evolution, $\Delta(t)$ (Eq.(16)), in the low-viscosity (τ_L / τ_{ther}=0.1) regime, with V=1 kJ/mol; the upper panel: E°=0, and the lower-panel $E^\circ + \lambda$=0. The cases of two smaller values of V, in the favor of Markovian nature, are demonstrated in the insert in each panel of this figure. A vertical shift on the evaluated $\Delta(t)$ in each insert is applied for the sake of clarity. For comparison, each evaluated $\Delta(t)$ is plotted together with its Kubo's $\Delta_K(t)$ and Markovian Δ_{Mar}=$\exp(-w_0 t)$ counterparts. The significant non-Markovian nature is observed in the upper-panel for the symmetric ET system with V=1 kJ/mol, where
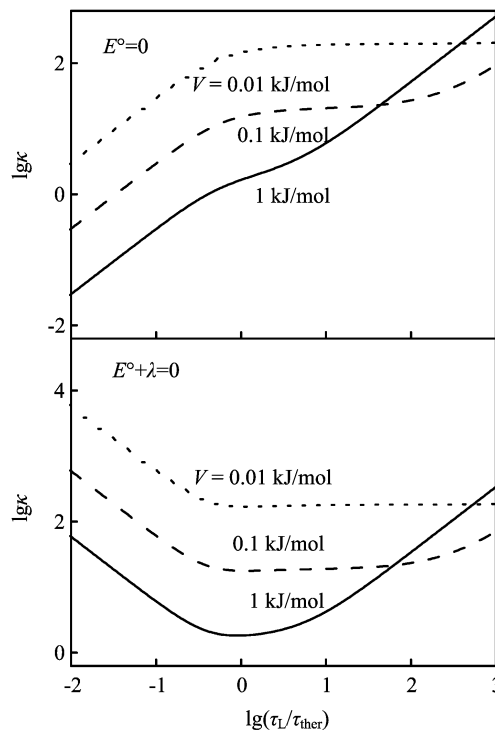

FIG. 2 The corresponding Markovianicity parameter κ (Eq.(21)) for each ET system in Fig.1.

the κ-parameter is found to be 0.3, agree well with the aforementioned approximate expression of Eq.(22).

B. Effect of solvation reorganization energy

We now examine the influence of solvent reorganization energy (λ) on the rate constant (k_0) and the Markovianicity parameter (κ). Figure 4 shows the $k_0 \sim \lambda$ curves for the specified three representing values of viscosity. Here $E^\circ = -3$ kJ/mol, V=1 kJ/mol, and T=298 K. The numerical evaluation is made on the basis of the continued fraction formalism of non-perturbative rate (the Eq.(36) with Eqs.(24)-(29) of Ref.[4]). It is verified again that the rate in the low-viscosity ($\tau_L < \tau_{ther}$) regime is nonadiabatic, with the maximum at λ_{max}=$|E^\circ|/(2k_B T \tau_L)$ (cf. Eq.(15)). In the high-viscosity ($\tau_L > \tau_{ther}$) regime, the rate is largely adiabatic. However, its maximum appears around $\lambda_{max} \approx -k_B T + \sqrt{(k_B T)^2 + (E^\circ)^2}$, i.e., its nonadiabatic counterpart of Eq.(14).

Figure 5 depicts the $k_0 \sim \tau_L$ curves for the three specified values of V, with λ=15 kJ/mol, $E^\circ = -3$ kJ/mol and T=298 K. Compared with the lower-panel of Fig.1, the ET systems in this figure are of the increased value of solvent reorganization energy. The observed $k_0 \sim \tau_L$ behavior in the low-viscosity regime here indicates clearly the interplay between quantum tunneling and barrier crossing (cf. both panels of Fig.1), with a turnover occurring at τ_L / τ_{ther}=$|E^\circ|/(2\lambda)$, as indicated in Eq.(15).
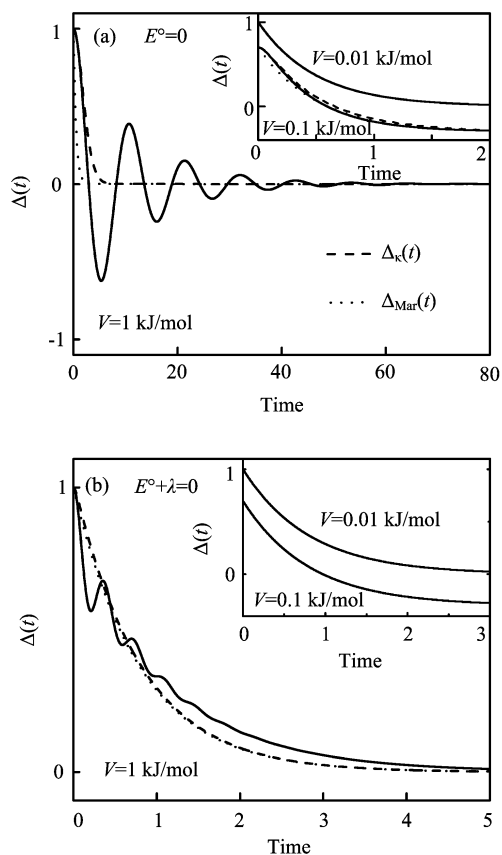
FIG. 3 The scaled population $\Delta(t)$(Eq.(16)), evaluated at $\tau_{\mathrm{L}}/\tau_{\mathrm{ther}}$=0.1, λ=3 kJ/mol, and T=298 K. The time variable is given in the unit of $1/k_0$ for each individual case. The results for the two smaller values of V are given in the insets, where a vertical shift is applied for clarity. Each $\Delta(t)$ is also associated with its Kubo's $\Delta_{\mathrm{K}}(t)$ (Eq.(20)) and Markovian $\Delta_{\mathrm{Mar}}(t)$ counterparts.

FIG. 4 The rate constant k_0 as function of the solvent reorganization energy λ, with the scaled relaxation time $\tau_{\mathrm{L}}/\tau_{\mathrm{ther}}$ specified along each curve, E°=–3 kJ/mol, V=1 kJ/mol, and T=298 K.

FIG. 5 The rate constant k_0 as function of the scaled solvent longitudinal relaxation time $\tau_{\mathrm{L}}/\tau_{\mathrm{ther}}$, with the transfer coupling strength V specified along each curve, E°=–3 kJ/mol, λ=15 kJ/mol, and T = 298 K.

Note that for the symmetric E°=0 system whose rate-viscosity dependence curve has been represented by the upper-panel of Fig.1, the $k_0\sim\lambda$ curve decays monotonically (not shown explicitly here). This is also consistent with the aforementioned λ_{max} expression.

Figure 6 and Fig.7 present the Markovianicity κ parameters associated with Fig.4 and Fig.5, respectively. For all the cases studied here, κ>1, implying the validity of Markovian rate constant description.

Figure 8 shows the resulting scaled population transfer, $\Delta(t)$ (Eq.(16)), of the ET system at T=298 K in the low-viscosity regime ($\tau_{\mathrm{L}}/\tau_{\mathrm{ther}}$=0.1), with λ=15 kJ/mol, E°=–3 kJ/mol and V=1 kJ/mol. The corresponding Markovianicity parameter κ=2.4. Those with two smaller values of V are plotted in the inset. Included in Fig.8 and its inset are also the corresponding Kubo's $\Delta_{\mathrm{K}}(t)$ (dashed) and Markovian Δ_{Mar}=exp($-w_0t$) (dotted) curves.
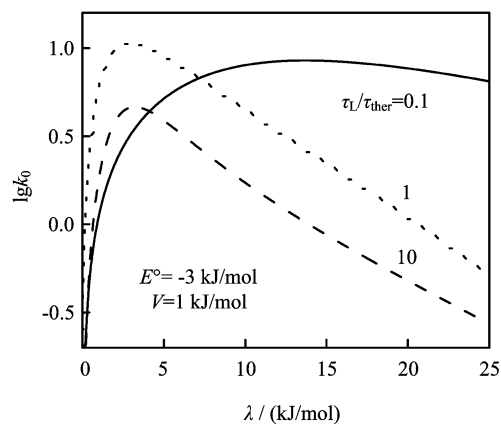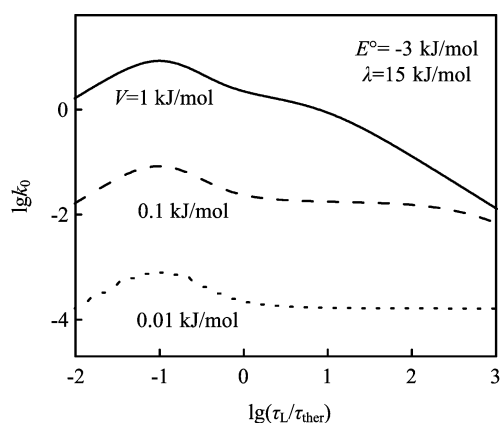
V. CONCLUSION

In conclusion, we have presented a Markovianicity parameter κ (Eq.(21)), based on the Kubo's motional narrowing line-shape function, to address the nature of electron transfer rate process. The solvent relaxation is typically in the order of picosecond, while τ_{ther} for room temperature is 26 fs. This amounts to the high-viscosity or slow-modulation regime of the present study. The resulting Markovianicity parameter, as depicted in Fig.2, Fig.6, and Fig.7, for its dependence on the involving parameters, illustrates why most experimental observations do support the Markovian (κ>1) rate constant description, i.e., Eq.(2) that leads to $\Delta(t)$=exp$[-(k_0 + k_0')t]$.

We have pointed out that a non-Markovian rate process is most likely to occur in the symmetric ET system at the fast-modulation (low-viscosity) regime. It is just the opposite to the spectroscopic case. According
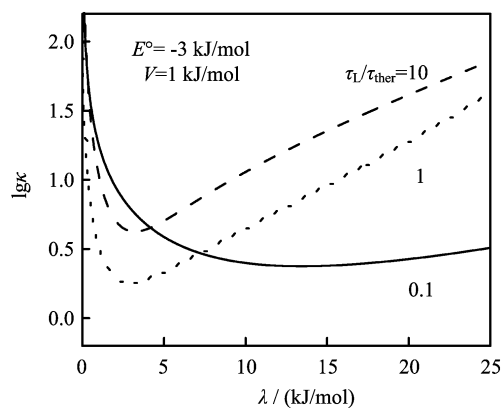
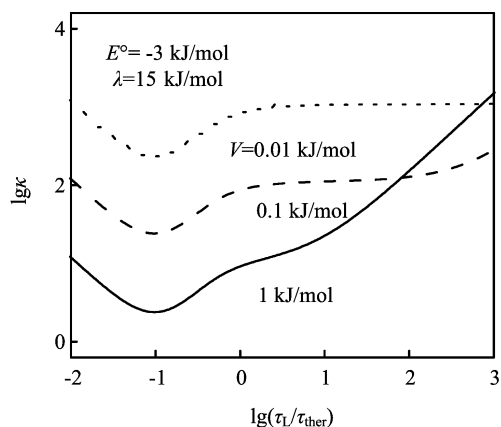FIG. 6 The corresponding Markovianicity parameter κ (Eq.(21)) for each ET system in Fig.4.

FIG. 7 The corresponding Markovianicity parameter κ (Eq.(21)) for each ET system in Fig.5.

FIG. 8 The scaled population $\Delta(t)$ (Eq.(16)), evaluated at $\tau_{\mathrm{L}}/\tau_{\mathrm{ther}}=0.1$, $E^\circ=-3$ kJ/mol, $\lambda=15$ kJ/mol, $V=1$ kJ/mol, and $T=298$ K. The time variable is given in the unit of $1/k_0$ for each individual case. The results for the two smaller values of V are given in the insets, where a vertical shift is applied for clarity. Each $\Delta(t)$ is also associated with its Kubo's $\Delta_{\mathrm{K}}(t)$ (Eq.(20)) and Markovian $\Delta_{\mathrm{Mar}}(t)$ counterparts.

to the motional narrowing picture, the fast modulation leads to a Markovian spectroscopic process [24,25]. The above seemingly counter-intuitive phenomenon in relation to the nature of rate process may be understood as follows. First of all, the motional narrowing picture is applied to the spectrum of rate kernel, rather than the population itself. The narrower the rate kernel spectrum is, the less Markovian the rate process would be. However, this is not the complete picture. The peak position of the rate kernel spectrum, in relation to where rate constant is evaluated, should also be considered. It shifts from the classical Marcus' inversion position at $E^\circ=-\lambda$ in the slow-modulation limit, to the quantum resonant tunneling at $E^\circ=0$ in the fast-modulation regime. Eq.(22) that is achieved at $E^\circ=0$ can be considered as the lower bound of the Markovianicity κ for the ET rate process in the fast modulation regime. Moreover, in the strong coherent transfer coupling regime, the population dynamics may also exhibit the quantum beat feature that is non-Markovian in a strict sense (cf. Fig.3).

The present demonstrations are made by using the Debye solvent model (Eq.(9)) with a semiclassical fluct-
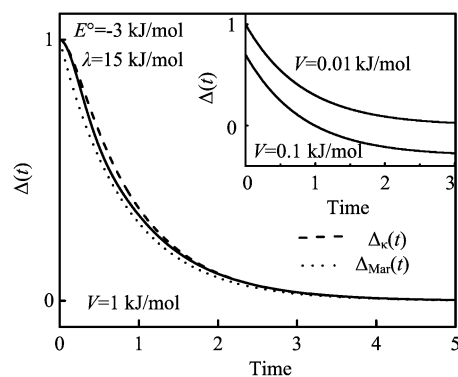
uation–dissipation theorem. This is the only approximation involved, valid when $k_{\mathrm{B}}T\gtrsim(V^2+E^{\circ 2}/4)^{1/2}$. The population dynamics and the rate constants are calculated on the basis of the hierarchical equations of motion and its equivalent continued fraction formalism constructed in Ref.[4], which are exact for the Debye solvent model used here. The nonadiabatic rate expressions presented in Section II are applicable to non-Debye solvents and used as the reference in the later discussions in Section IV. Also note that the Debye model contains only a single dielectric relaxation time constant. A realistic solvent usually consists of multiple time parameters, which generally enter the rate theory in a nonlinear manner, especially in the strong transfer-coupling regime at low temperature. We shall investigate this complex case elsewhere.

VI. ACKNOWLEDGMENTS

[1] M. Sparpaglione and S. Mukamel, J. Chem. Phys. **88**, 3263 (1988).

[2] M. Sparpaglione and S. Mukamel, J. Chem. Phys. **88**, 4300 (1988).

[3] Y. J. Yan, M. Sparpaglione, and S. Mukamel, J. Phys. Chem. **92**, 4842 (1988).

[4] P. Han, R. X. Xu, B. Q. Li, J. Xu, P. Cui, Y. Mo, and Y. J. Yan, J. Phys. Chem. B **110**, 11438 (2006).

[5] P. Han, R. X. Xu, P. Cui, Y. Mo, G. Z. He, and Y. J. Yan, J. Theor. Comput. Chem. **5**, 685 (2006).

[6] A. Nitzan, *Chemical Dynamics in Condensed Phases: Relaxation, Transfer and Reactions in Condensed Molecular Systems*, New York: Oxford University Press, (2006).

[7] R. A. Marcus, J. Chem. Phys. **24**, 966 (1956).

[8] R. A. Marcus, Annu. Rev. Phys. Chem. **15**, 155 (1964).

[9] R. A. Marcus and N. Sutin, Biochim. Biophys. Acta **811**, 265 (1985).

[10] L. D. Zusman, Chem. Phys. **49**, 295 (1980).

[11] L. D. Zusman, Chem. Phys. **80**, 29 (1983).

[12] J. T. Hynes, Annu. Rev. Phys. Chem. **36**, 573 (1985).

[13] A. Garg, J. N. Onuchic, and V. Ambegaokar, J. Chem. Phys. **83**, 4491 (1985).

[14] H. Frauenfelder and P. G. Wolynes, Science **229**, 337 (1985).

[15] P. G. Wolynes, J. Chem. Phys. **86**, 1957 (1987).

[16] M. Sparpaglione and S. Mukamel, J. Phys. Chem. **91**, 3938 (1987).

[17] Y. J. Yan and S. Mukamel, J. Phys. Chem. **93**, 6991 (1989).

[18] S. Mukamel and Y. J. Yan, Acc. Chem. Res. **22**, 301 (1989).

[19] J. Tang and S. H. Lin, J. Chem. Phys. **107**, 3485 (1997).

[20] M. Bixon and J. Jortner, Adv. Chem. Phys. **106**, 35 (1999).

[21] N. R. Kestner, J. Logan, and J. Jortner, J. Phys. Chem. **78**, 2148 (1974).

[22] R. X. Xu and Y. J. Yan, Phys. Rev. E **75**, 031107 (2007).

[23] J. S. Jin, S. Welack, J. Y. Luo, X. Q. Li, P. Cui, R. X. Xu, and Y. J. Yan, J. Chem. Phys. **126**, 134113 (2007).

[24] R. Kubo, Rep. Prog. Phys. **29**, 255 (1966).

[25] R. Kubo, Adv. Chem. Phys. **15**, 101 (1969).

[26] H. A. Kramers, Physica (Amsterdam) **7**, 284 (1940).

[27] P. Hänggi, P. Talkner, and M. Borkovec, Rev. Mod. Phys. **62**, 251 (1990).